Characterizing the Spatial Distribution of Coral Reefs in the South-Central Coast Region of Vietnam using Planetscope Imagery

Khanh V. Nguyen[1], Vinh C. Duong[2], Kinh T. Kieu[1], Thuong V. Tran[3*], Cho-ying Huang[4], Ruth Reef[5], Thien M. Hoang[1]

[1] Faculty of Biology and Environment, University of Science and Education, The University of Danang, Danang city, Viet Nam.
[2] Department of Environment and Natural Recourses, Gia Lai Campus, Nong Lam University – Ho Chi Minh, Gia Lai province, Viet Nam.
[3] Institute of Engineering and Technology, Thu Dau Mot University, Binh Duong province, Viet Nam.
[4] Department of Geography, National Taiwan University, Taipei, Taiwan.
[5] School of Earth, Atmosphere and Environment, Monash University, Clayton, Victoria, Australia

Corresponding Author: Thuong V. Tran[*]
No. 6, Nguyen Van On street, Thu Dau Mot city, Binh Duong province, 75000, Viet Nam.
Email address: thuong.tran@tdmu.edu.vn

Abstract

This study aims to understand the spatial distribution of coral reefs in the central region of Viet Nam. We classified live coral cover in Son Tra Peninsula (ST) and Cu Lao Cham Island (CLC) in the South-Central Coast Region of Viet Nam using the Maximum Likelihood Classifier on 3 m Planetscope imagery. Confusion matrices and the accuracy of the classifier were assessed using field data (1,543 and 1,560 photographs in ST and CLC, respectively). The results showed that the reef's width ranged from 30 to 300 m across the study site, and we were able to detect live coral cover across a depth gradient of 2 to 6 m below the sea surface. The overall accuracies of the classifier (the Kappa coefficient) were 76.78% (0.76) and 78.08% (0.78) for ST and CLC, respectively. We found that 60.25% of coral reefs in ST were unhealthy and the live coral cover was less than 50%, while 25.75% and 11.46% of those in CLC were in good and excellent conditions, respectively. This study demonstrates the feasibility of utilizing Planetscope imagery to monitor shallow coral reefs of small islands at a high spatial resolution of 3 m. The results of this study provide valuable information for coral reef protection and conservation.

Introduction

39 Coral reefs make up only 0.1% of the global ocean substrate, yet they are one of the most
40 biodiverse marine ecosystems and they play a key role in providing a range of ecosystem services
41 (Hoegh-Guldberg, Pendleton & Kaup, 2019; Obura et al., 2019; Pawlik & McMurray, 2020).
42 Southeast Asia contains the largest area of coral reef cover on Earth, estimated at 91,700 km^2,
43 followed by the Australia - Papua New Guinea region at 62,800 km^2 (Guan et al., 2020). Coral
44 cover in the SE Asia region has declined and is being threatened by both local and global stressors
45 such as marine pollution and runoff, direct destruction, overexploitation of key species, outbreaks
46 of coral predators, and climate change (Zhou et al., 2018; Hoegh-Guldberg, Pendleton & Kaup,
47 2019; Carriger, Yee & Fisher, 2021). Long term monitoring programs of coral health in the SE
48 Asia region are important for managing this global biodiversity hotspot which is facing a range of
49 impacts (Tun et al., 2008), Characterize coral reef cover and health over large spatial and temporal
50 scales is critical for the effective management and protection of coral reef resources (McCarthy et
51 al., 2017; Zhou et al., 2018). The use of remote sensing to monitor reefs over large temporal and
52 spatial scales will be necessary to provide standardized data for reef health across the SE Asian
53 region over this period of rapid change and population growth.

54

55 Coral reef monitoring applies both quantitative measurements to explore area coverage of basic
56 reef bottom-types (e.g., coral cover), and provides information about coral reef health. These
57 monitoring frameworks are designed to develop effective strategies for management, conservation,
58 and restoration of coral reefs across various spatial scales (Guan et al., 2020; Carriger, Yee &
59 Fisher, 2021). Coral coverage and health is conducted using two primary approaches including *in-
60 situ* surveys and remotely sensed data (Hedley et al., 2016, 2018; McCarthy et al., 2017; Gonzalez-
61 Rivero et al., 2020). *In-situ* methods provide a high resolution images from a handle camera and
62 compositionally detailed quantitative description of coral reef biodiversity, through SCUBA driver
63 surveys (e.g., underwater geo-located digital photography) or high resolution aerial images that
64 are costly and time consuming (Levy et al., 2018; Li et al., 2019). Thus, while *in-situ* methods can
65 provide unrivaled detail on species diversity, coral density, and individual colony size and health;
66 the spatiotemporal scale of these analyses is limited and biased against remote reefs, periods of
67 severe weather conditions, or challenging reef topography (Levy et al., 2018). Satellite remote
68 sensing to acquire coral information at different scales has been a cost-effective alternative or
69 complement for *in-situ* surveys (Hedley et al., 2018; Levy et al., 2018; Zhou et al., 2018; Li et al.,
70 2019). Among various sensors, the medium spatial resolution (30 m) Landsat images has been the
71 most widely used for regional mapping coarse coral habitat classes (e.g., 04 classes) (Tobler, 1988;
72 Zhou et al., 2018). Recently, freely available (for education and research programs) high spatial
73 resolution (3 m) Planetscope imagery has demonstrated potential in coral pattern observation
74 providing daily images (Lemajic, Vajsová & Aastrand, 2018; Lazuardi, Wicaksono & Marfai,
75 2021; Mansaray et al., 2021; Wulandari & Wicaksono, 2021).

76

77 Viet Nam has a large marine area with over 3,260 km of coastline and more than 3,000 islands
78 (Nguyen & Nguyen, 2014). The distribution of coral reefs in Viet Nam is along the coast and
79 around offshore islands, and is categorized into five separate regions (i.e., western Tonkin Gulf,
80 Middle-central, South-central, South-eastern, and South-western) (Hedberg et al., 2017). The
81 highest coral diversity is in the South-Central area (SCA) with 400 coral species recorded (i.e.,
82 Son Tra Peninsula [ST], Da Nang, Cu Lao Cham Island [CLC], Nha Trang, and Ninh Hai)
83 (Latypov & Selin, 2008; Nguyen & Vo, 2013). However, the health of coral reefs (as defined by
84 live coral cover) in the SCA has noticeably declined in the past few decades, with the condition of
85 ~50% of the reefs in this region currently classified as poor/very poor and only 11.6% and 2.9%
86 of the reefs classified as being in good and excellent conditions, respectively (Nguyen & Phan,
87 2008; Nguyen, 2009; Nguyen & Vo, 2013). Previous studies utilized various medium and high
88 spatial resolutions satellite data such as Landsat, SPOT-5, GeoEye-1, IKONOS, QuickBird, and
89 VNRedsat-1 to map general reef bottom-types, coral coverage, and reef building or expansion in
90 this region (Tran, Phinn & Roelfsema, 2012; Nguyen, Luong & Ho, 2015; Nguyen, Bui & Nguyen,
91 2019; Nguyen et al., 2019a). However, these studies have not examined the spatial distribution of
92 reef health (live coral cover). Therefore, the objectives of this study were: (i) to utilize Planetscope
93 imagery, a free satellite for education and research programs, for determining coral reef types at a
94 high spatial resolution; (ii) to understand spatial distribution of coral reef categories (i.e., live coral
95 cover and classification of benthic categories) in ST and CLC in the South-Central area of Viet
96 Nam.
97

Materials & Methods

99 **Study sites**
100 The study areas (i.e., ST [108°13'58.1"E-16°08'54.4"N and 108°20'22.4"E-16°05'16.2"N] and
101 CLC [108°24'42.8"E–15°58'57.7"N and 108°33'04.2"E-15°53'58.4"N]) are nature reserve areas
102 located in the South-central coast region of Viet Nam (Nguyen, Huynh & Zhang, 2015; Hoang et
103 al., 2019) (Figure 1). CLC was recognized as a world biosphere reserve by UNESCO in 2009
104 (Nguyen, Huynh & Zhang, 2015). The study sites are located within the tropical monsoon region
105 with a distinct dry season (January-July) receiving 600 mm rainfall over these 6 months and a
106 rainy season, where 80% of the annual rainfall (2,000 mm) falls between the month of August to
107 December. The annual mean temperature at the study areas is about 26°C with little seasonal
108 variation. The region is regularly disturbed by typhoons and river run-off in the wet season, which
109 can lead to destruction of reefs.
110

111 **Figure 1.** Location of study area (a) Son Tra Peninsula (ST) and (b) Cu Lao Cham Island (CLC).
112

113 The reefs at study area are shallow fringing reefs, with a diversity of 226 and 227 coral species in
114 ST and CLC, respectively (Kimura, Tun & Chou, 2014, 2018). Deposited materials on the ocean
115 floor in this region is sand and rubble, which deposit between the inner and outer reef regions.
116 Both regions are important to their local economies providing revenue from coral reef-based

117 tourism, and small-scale fisheries. However, these reefs are under threat from an accumulation of
118 stressors such as human disruption, typhoons, new outbreaks of crown of thorns starfish, excess
119 terrigenous sediment output due to land use change, pollution, overfishing, destructive fishing, and
120 the mining of reefs for limestone (Nguyen & Vo, 2013; Quach, 2018). A lack of regular monitoring
121 has impacted on effective coral reef management and protection (Le, 2020).
122
123 **Data collection and Processing**
124 The Planetscope images (3 m spatial resolution) used in this study were obtained from the Planet
125 Education and Research Program server (https://www.planet.com/markets/education-and-
126 research/) (Table 1). The wavelengths of Planetscope imagery cover the blue (455 – 515 nm),
127 green (500 - 590 nm), red (590 – 670 nm), and near-infrared (780 - 860 nm) spectral regions (Gabr,
128 Ahmed & Marmoush, 2020). These images were acquired on 28 June 2019 (ST) and 08 August
129 2019 (CLC) with 0% of cloud cover and coordinate system projection of WGS 84/ UTM zone
130 49N. The images, acquired by a Dove satellite with additional postprocessing applied, known as
131 the PlanetScope Ortho Scene Product (level 3B), were ortho-rectified, atmospherically corrected,
132 and scaled to surface reflectance (Lemajic, Vajsová & Aastrand, 2018).
133
134   **Table 1**. Details of the acquired Planetscope imagery
135
136 We carried out field surveys during August and September 2019 to gather information about the
137 depth and features of the ocean bottom. The bottom features were measured following the 25's
138 method, proposed by (Roelfsema, Phinn & Joyce, 2006), in a grid of 5 m x 5 m using an underwater
139 camera (GoPro HERO 8, USA). Based on this approach, five photographs including the four
140 corners and one center positions of a 1 m x 1 m quadrat were taken. The underwater photographs
141 were ortho-rectified to control the spatial uncertainty to < 3 m in order to match the resolution of
142 the satellite data. The depth and the coordinates of each photograph were recorded using a Hondex
143 PS-7FL (Honda Electronics Ltd., Toyohashi, Japan) and Garmin GPS MAP 62sc (Garmin Ltd.,
144 Lenexa, Kansas, USA), respectively. In addition to photo capture in the 5 x 5 m grid, underwater
145 360 video transects (CND713, CND Co., Ltd., Korea) were taken to determine the ocean floor
146 classes (Table 2) in deep and homogenous areas before collecting substrate types (i.e., sand, and
147 hard bottom) to reduce the cost of field survey. A total of 1,543 photographs and 167 video
148 transects at ST and 1,560 photographs and 174 video transects at CLC were collected during the
149 field campaign. The photos were filtered to select for good quality photographs demonstrating
150 their ability to clearly identify the bottom feature. Five photographs were overlapped to create a
151 transect and each transect was geo-referenced based on captured coordinates before analyzing the
152 benthic composition by the Coral Point Count Excel (CPCe) software (Kohler & Gill, 2006;
153 Roelfsema, Phinn & Joyce, 2006).
154
155 Bottom types, derived from the photographs of 1 x 1 m quadrats, were identified into four classes
156 (i.e., live coral [hard and soft coral], sand, hard bottom [rock, rubble, dead coral], deep water [>

157   14 m]) (Hill & Wilkinson, 2004), and were used to calculate proportion of substrate composition.
158   The coral reef health in 5 x 5 m grids was categorized as the 'poor', 'fair', 'good' or 'excellent'
159   condition based on live coral cover (Chou et al., 1995; Hill & Wilkinson, 2004) (Table 2). Finally,
160   a part of the ground-truth samples was randomly selected for image classification training (see the
161   sub-section in Supervised classification and coral cover mapping). A total of 323 and 369
162   randomly selected ground-truth samples in the ST and CLC, respectively, were identified to assess
163   classification accuracy. It included each classed category as follow: 1LC (69), 2LC (64), 3LC (47),
164   HB (43), S (51), and D (49) in Son Tra and 1LC (62), 2LC (56), 3LC (54), 4LC (55), HB (43), S
165   (55), and D (44) in Cu Lao Cham. (Table 2 and the Data Supplemental Files).
166
167   **Table 2.** Identification scheme of bottom types and coral reef health
168
169   **Sun glint correction and water column correction**
170   Sun glint occurs in images under conditions of clear skies, shallow waters (when wind generated
171   waves disturb the surface), more so when images are acquired at a high spatial resolution (Hedley,
172   Harborne & Mumby, 2005). This phenomenon could be defined as the specular reflection of light
173   from the water surface, when the component of sensor-received radiance due to the surface
174   reflection is greater than the water-leaving radiance from sub-surface features (Kay, Hedley &
175   Lavender, 2009). Previous studies proposed sun-glint removal methods for ocean color
176   applications with resolutions on the scale of 100–1,000 m (Wang & Bailey, 2001; Hedley,
177   Harborne & Mumby, 2005; Kay, Hedley & Lavender, 2009). However, these models could only
178   correct moderate glint and large errors remain in the brightest glint areas (Kay, Hedley &
179   Lavender, 2009). Hence, a separate set of revised methods were developed for benthic remotely
180   sensed data at high spatial resolutions (<10 m) (Hochberg, Andréfouët & Tyler, 2003; Kay, Hedley
181   & Lavender, 2009). These approaches use data from the near-infrared (NIR) to determine the
182   amount of glint in the received signal (Hedley, Harborne & Mumby, 2005; Kay, Hedley &
183   Lavender, 2009), thus improving data retrieval for bathymetry or coral habitat classification
184   (Hochberg, Andréfouët & Tyler, 2003; Hedley, Harborne & Mumby, 2005; Kay, Hedley &
185   Lavender, 2009). In this study, the sun light correction of the Planetscope images were undertaken
186   using a revised 'de-glinting' method (Hochberg, Andréfouët & Tyler, 2003; Hedley, Harborne &
187   Mumby, 2005). Following this approach, the relationships between NIR and visible bands were
188   explored by linear regression based on a sample of the image pixels. The pixel sample was
189   collected from one or more region of the image where a range of sun glint is evident, but where
190   the underlying spectral brightness would be expected to be consistent (normally deep-water areas)
191   (Hedley, Harborne & Mumby, 2005). If the slope of the regression line for band i is b_i, then all
192   pixels in the image could be de-glinted in band i, following Equation (1):
193

$$L'_i = L_i + b_i(L_{NIR} - Min_{NIR}),$$ (1)

194

195 where, L'i is the de-glinted pixel of visible band i; L_i is reflectance from visible band i; b_i is the
196 regression slope; L_{NIR} is reflectance from NIR band; and Min_{NIR} is minimum value of NIR band.
197

198 In addition to the sun glint phenomenon, we needed to correct for the water column so that bottom
199 classes were not misclassified due to different water column conditions (Zoffoli, Frouin & Kampel,
200 2014). Among various algorithms, Lyzenga's equation (Lyzenga, 1978, 1981) is widely applied to
201 empirically diminish water column attenuation impacts. This method enhances mapping accuracy
202 in digital classification processes of bottom types, and does not require knowing the local depth
203 across every pixel of the scene (Green et al., 2000; Pahlevan, Valadanzouj & Alimohamadi, 2006;
204 Pu et al., 2012; Zoffoli, Frouin & Kampel, 2014). The algorithm uses multispectral image datasets
205 to generate 'depth – invariant' coefficients of bottom types from each pair of spectral bands. The
206 result of the correction creates multiple 'depth - invariant bands, replacing original bands to classify
207 bottom features (Green, Mumby, Edwards, & Clark, 2000). The depth-independent composition
208 of corrected radiance (DII_{ij}) in bands i and j (pseudo-color band) was generated by Equation (2):

$$DII_{ij} = \ln(L_i) - \left[\left(\frac{k_i}{k_j} \right) \ln(L_j) \right],$$ (2)

209 Where L_i is de-glinted pixel of band i; L_j is de-glinted pixel of band j; $\left(\frac{k_i}{k_j} \right)$ is the ratio of
210 attenuation coefficients.
211 In this study, three visible bands of PlanetScope imagery with high water penetration were plotted
212 against transformed band pairs (i.e., band 1 and band 2, band 2 and band 3, band 1 and band 3).
213 The slope values of the ratio of attenuation coefficients for each band were applied to generate
214 three DII bands (i.e., DII_{12}, $DII_{13,}$ and DII_{23}) to class the bottom types.
215

216 **Supervised classification and coral cover mapping**
217 Different types of supervised classification methods have been used to identify coral reefs with
218 water column corrected images and bottom classes in similar marine regions. The Maximum
219 Likelihood Classifier was used due to its effectiveness and adaptability, compared to other
220 classifiers (Ali, Qazi & Aslam, 2018; Cabral et al., 2018). In the current study, the Maximum
221 Likelihood Classifier was subsequently applied to each image. This classifier was based on a
222 probability density function and guessed the probability with which a specific pixel belongs to a
223 specific category (Richards, 1999).The standard false colour satellite images were composed
224 before applying the supervised classification approach. The standard implementation of supervised
225 maximum likelihood classification required training samples representing the feature types to be
226 classified (Lillesand, Kiefer & Chipman, 2015). Taking this *a-priori* knowledge into account, each
227 pixel was labelled as 1LC, 2LC, 3LC, 4LC, HB, S and D (Table 2). Finally, we used a 3 × 3 focal
228 majority filter to minimize the "salt-and-pepper effect" in the coral reef maps (Booth & Oldfield,
229 1989).
230

231 Finally, to validate the classification results, an error matrix was produced to assess the
232 performance. We used independent training sites to assess the accuracy of each classification. The
233 error matrix showed seven classes using four metrics: overall accuracy (OA), producer's accuracy
234 (PA), user's accuracy (UA), and the Cohen Kappa coefficient. The Kappa coefficient was
235 computed using equation (3):

236

237 $$K = \frac{Observed\ Accuracy\ -\ Change\ Agreement}{1 - Change\ Agreement} \tag{3}$$

238 The Kappa coefficient measures the agreement between the classification and ground-truth values.
239 A Kappa value of 1 represents perfect agreement, while a value of 0 represents no agreement. We
240 interpreted the Kappa values as per Table 3 following (McHugh, 2012; Nguyen, Luong & Ho,
241 2015). All the image processing and post-classification steps, presented in Figure 2, were
242 processed using ArcGIS v. 10.8 software packages (ESRI, USA).

243

244   **Table 3.** Interpretation of Kappa values

245

246   **Figure 2.** Flowchart of coral distribution mapping in the study area

247

248 ## Results

249 **Descriptive field data analysis**

250

251 The correlation coefficients and ratio of attenuation coefficients among visible bands at good water
252 penetration (Figure 3). To perform the water column correction, homogenous sand substrates of
253 varying depths collected from field surveys were applied to calculate the ratio of attenuation
254 coefficients. The very high correlation coefficients of 0.95 above were explored between bands 1
255 and 2, while the relationship between bands 1 and 3 showed high R^2 values of 0.85 in both ST and
256 CLC.

257

258 **Figure 3.** Transformed band ratios of Planetscope bands in ST [(a) bands 1 and 2, (b) bands 2
259 and 3, and (c) bands 1 and 3] and in CLC [(d) bands 1 and 2 (e) bands 2 and 3, and (f) bands 1
260 and 3]

261

262 In addition to the water column correction, the study analyzed the spectral signatures among the
263 bottom types (i.e., coral lives and non-coral classes) based on 04 visible bands after corrected sun
264 glint. Many studies measured the spectral characteristics from *in situ* data or from remotely sensed
265 data (Green et al., 2000; Hochberg, Andréfouët & Tyler, 2003; Yamano & Tamura, 2004; Leiper
266 et al., 2014; Giardino et al., 2019). These studies considered that separating spectral features
267 among coral reef bottom classes is challenging. The classes with good separation are sand
268 dominated vs deep water classes representing light and dark objects, respectively (Green et al.,
269 2000; Hochberg, Andréfouët & Tyler, 2003). Our analysis shows that good discriminating ability

270   is also found between the D and S classes, while HB bottom easily overlapped with 1LC and 2LC
271   classes in the blue and green bands in both study areas. For live corals, the spectral characteristics
272   utilized a separation among bands blue, red, and NIR (Figure 4). The reflectance of bottom types
273   among these classes decreased in the blue to red bands while increasing at the NIR band.
274   Therefore, the high separation among bands permits the classification of live coral and bottom
275   types in both areas.
276
277   **Figure 4**. Spectral signatures of (a) six classes at ST and (b) seven classes at CLC
278
279   **The patterns of coral reefs distribution**
280   From the analysis of field survey results, the most common coral reef types in the study areas were
281   fringing reefs, reefs directly attached to the shoreline of the peninsula and the islands. This reef
282   type varied in relation to a combination of coastline geomorphology and seabed characteristics,
283   normally ranging between 30 and 300 m in width. The vertical pattern of coral distribution in the
284   study area reached to 14 m in depth and was densest between 2 and 6 m (Figure 5).
285
286   **Figure 5.** Depth histogram of coral distribution in (a) Son Tra Peninsula and (b) Cu Lao Cham
287   Island.
288
289   The depth distribution of coral reefs and other substrates is presented in Figures 6 and 7 for ST
290   and CLC, respectively. Coral reefs in ST were located along the shoreline from Tien Sa in the
291   northwest to Hon Sup in the southwest. The northwestern most coral reefs in this region were not
292   included in this study due to the high turbidity of the Han estuary. High coral cover was found in
293   the inner coral reefs of the northern ST, while coral cover was patchier in the southern region as
294   shown by the alternating distribution of three classes (1LC, 2LC and 3LC; poor, fair, and good
295   coral cover respectively) across the reef (Figure 6). In southwest ST including Bai Nom, Bai But,
296   and Hon Sup (Figure 6d-e), the reef width ranged between 140 – 300 m, while across the rest of
297   ST reefs were narrower (30 – 90 m wide).
298
299   **Figure 6.** Coral cover in Son Tra Peninsula (i.e., 1LC: Poor; 2LC: Fair; 3LC: Good; S: Sand; and
300   HB: Hard bottom).
301
302   In CLC, coral reefs were located throughout the western and northern shores of Hon Lao (main
303   island) and around small islands (i.e., Hon Kho, Hon La, Hon Mo, Hon Tai, and Hon Dai) (Figure
304   7a, b, g, and h). High coral cover was found predominantly in the southern part of the smaller
305   islands, while the northern shores of the islands recorded lower coral cover (Figure 7). The widest
306   reef (150 m) was the SunGroup reef (near the tourist area managed by SunGroup) while the reef
307   width at the rest of the island locations ranged between 50–100 m.
308

309 **Figure 7.** Coral cover in Cu Lao Cham Island (i.e., 1LC: Poor; 2LC: Fair; 3LC: Good; 4LC:
310 Excellent; S: Sand; and HB: Hard bottom).

311

312 Following the classification of the bottom cover into different categories (Table 2), we estimated
313 that the live coral areas were 0.47 km^2 and 0.58 km^2 in the ST and CLC, respectively. Bottom
314 cover proportion is reported in Table 4. In ST, the health condition of ranged from 'poor' to 'fair
315 condition' with 60.25% classified as a coral reef in poor condition (1LC), 31.88% in 'fair
316 condition' (2LC), and only 7.87% in 'good condition' (3LC). Several regions (e.g., Vung Da Ban
317 and Tay Bai Bac - Dong Bai Bac) recorded over 70% of coral cover in poor condition, while none
318 of the reefs were in good condition or above.

319

320 Compared to ST, the health condition of coral reefs in CLC was better and more consistent across
321 reefs. Despite the better condition, the percentage of reefs in poor health still accounted for
322 34.28%, followed by 2LC and 3LC at 28.51% and 25.75%, respectively. However, the proportion
323 of coral reefs in 'excellent condition' in the CLC was 11.46%, compared to none in the ST. This
324 is perhaps due to several programs to protect and recover coral reefs in the CLC (Hua et al., 2015;
325 Quach, 2018) such as the reef recovery program at some regions of Cu Lao Cham Island (e.g., Hon
326 Tai, Hon La and Hon Dai, Bai Bac and Bai Huong), which have contributed to coral reef health
327 (Hua et al., 2015).

328

329 **Table 4.** Percentage of coral cover classes in the coral reefs of Son Tra Peninsula and Cu Lao
330 Cham Island

331

332 **Performance assessment**
333 The Planetscope images provided three visible spectral bands that enabled us to penetrate to the
334 water bottom and perform the classification of the benthos (Green et al., 2000; Mumby et al., 2004)
335 and a NIR band that we used for sun-glint removal, subsequently improving the classification
336 accuracy (Hedley, Harborne & Mumby, 2005; Anggoro, Siregar & Agus, 2016). Assessments of
337 accuracy were carried out on the coral cover and bottom classes by comparison with geo-rectified
338 ground reference data collected during field surveys. Error matrices were generated for each of the
339 classified images in ST and CLC (Tables 5 and 6, respectively). The overall classification
340 accuracies (Kappa coefficients) for ST and CLC were 78.08% (0.78) and 76.78% (0.76),
341 respectively. Among the various coral and bottom types, deep zone and sands class showed the
342 highest producer's accuracies (PA) and user's accuracy (UA) in both regions because of both the
343 exponential decrease of light intensity with increasing depth and the high light absorption through
344 the column before reaching to the deep bottom (Green et al., 2000; Goodman, Purkis & Phinn,
345 2013). In the coral cover classification, the highest PA (78.57%) and UA (80.85%) were found for
346 2LC and 3LC, respectively in ST, followed by the 1LC at 76.56% and 71.01%, respectively.
347 Whereas these indicators were quite different in CLC. Major areas of confusion and

348   misinterpretation were found to roughly coincide with the transitional areas between hard bottom
349   (HB) and coral classes.
350
351   **Table 5.** Confusion matrix of bottom types in Son Tra Peninsula
352
353   **Table 6.** Confusion matrix of bottom types in Cu Lao Cham Island
354
355

Discussion

357   Coral reef health in almost regions of Viet Nam is declining due to land use conversion at coastal
358   and marine areas under the pressure of economic development (Nguyen & Nguyen, 2014; Nguyen
359   et al., 2019). Monitoring and detecting coral reefs plays a crucial role in proposing natural resource
360   management policy, environmental management, and conservation efforts (Asner, Martin &
361   Mascaro, 2017). Using remote sensing tools can address the coral reef health knowledge gap for
362   much of the region. However, the performance remotely sensed image classification depends on
363   the relationship between the spatial resolution of remotely sensed data and the number of
364   categories in the classification (Mumby & Edwards, 2002; Capolsini et al., 2003; Wicaksono &
365   Lazuardi, 2018; Li et al., 2019). For example, Wicaksono & Lazuardi, (2018) presented a range of
366   Kappa values of 0.21 - 0.40 by using Planetscope (3 m) for mapping benthic habitat and seagrass
367   species in Karimunjawa Islands with five classes, while a higher Kappa value of 0.81 was found
368   in Li et al., (2019) by using Dove (3 m) satellite data to map coral reef habitats in marine the
369   sanctuary Arrecifes del Sureste. Therefore, the selection of adaptive data for coral observation at
370   the region scale was highlighted in this study. The visualization of PlanetScope data for mapping
371   the spatial distribution of benthic community has also been confirmed by recent studies in Viet
372   Nam (Nguyen et al., 2019, b). The first study in Viet Nam using Planetscope images to monitor
373   submerged aquatic vegetation (5 classes) showed a high overall accuracy and Kappa coefficient at
374   92.52% and 0.90, respectively (Nguyen et al., 2019). Therefore, with 07 classification categories,
375   the Kappa coefficients and the overall accuracy in our study indicate sufficient accuracy for post
376   classification assessment.
377
378   In addition to Planetscope images, previous studies applied other sensors to explore coral
379   distribution in Viet Nam. For example, Tran, Phinn & Roelfsema, (2012) used images of IKONOS
380   (3.2 m), QuickBird (2.4 m), and GeoEye-1 (5 m) for categorizing benthic cover. More recently,
381   Nguyen, Luong & Ho, (2015 and Nguyen, Bui & Nguyen, (2019) applied medium resolution
382   satellite images [e.g., Landsat 8 OLI (30m), SPOT-5 (10m)] for coral mapping in Ly Son island
383   and Nam Yet island, respectively. However, these studies were only characterized coral cover to
384   other benthic cover and bottom types and unclassified or divided coral lives into separate class.
385   Hence, findings in this study are one of the very first studies applying the Planetscope imagery for
386   monitoring coral cover patterns with 04 coral live classes in the South-Central Coast of Viet Nam.
387   Besides, the outcomes in our study were comparable to those of Capolsini et al., (2003) and Phinn,

388 Roelfsema & Mumby, (2012) that used commercial Quickbird-2 (2.4 m), WorldView-2 (0.5 m),
389 and IKONOS (3.2 m) images, respectively to explore coral reefs. Here we affirm the potential of
390 Planetscope imagery for visualizing higher resolution coral health monitoring metrics. This
391 approach is expected to provide managers with more accurate data, reduce time, manpower and
392 cost in marine conservation in developing countries.
393
394 We mapped coral distribution in ST and CLC as a case study of the South-Central Coast region in
395 Viet Nam. However, some limitations have been discovered. Offsets associated with the difference
396 between the actual positions and field locations when a scuba diver took underwater photos and
397 GPS estimates from the surface reduced spatial certainty to 5 X 5. Hence, around deep-water areas
398 (15 m depth) especially where the bottom morphology is narrow, each photograph covered an area
399 over 5 m², reducing the number of field images for bottom feature identification. Besides, around
400 the field sites with homogenous bottom characteristics (i.e., sand, hard bottom, and deep water),
401 individual photos and the camera of 360 CND713 were used to record the bottom, to identify
402 neighboring areas, and to enhance the ground truth data for the D class. Therefore, the number of
403 filtered and random ground truth data to perform error matrix for post classification in this study
404 reduced.
405
406 For future research, a time-series of PlanetScope images should be obtained and applied to explore
407 the spatiotemporal pattern of coral reef variation. Besides, intersection between coral pattern and
408 various information layers (e.g., geology, climatic condition, biomes, land use and land cover
409 change) should be employed to better understand distribution and diversity and to propose
410 strategies for coral conversation. Nonetheless, optimizing the data collection and analysis related
411 to classification and field survey methods should be compared to enhance accuracy assessment.
412
413 **Conclusions**
414 The distribution of coral reefs (coral cover and bottom types) in ST and CLC in the South-Central
415 Coast of Viet Nam was characterized using very high spatial resolution (3 m) Planetscope imagery
416 with a supervised classification approach. Seven classes, including coral reef health (04 classes)
417 and bottom types (03 classes), were categorized to determine coral cover and condition of the reefs
418 in the study area. Field surveys of 1,543 photographs in ST and 1,560 photographs in CLC were
419 used to assess accuracy.
420
421 The study characterized coral reefs distribution and health in a peninsula setting and offshore
422 islands. The results revealed that the overall condition of coral reef was of 'poor condition' in the
423 Son Tra (60.25%) and ranged between 'fair and good condition' in CLC. Additionally, the reefs
424 in both areas were predominantly fringing reef, reaching a depth of 14 m and a width of 400 m. In
425 ST, there were better environmental conditions in the southern area than in the northern area which
426 was indicated by the higher density of live coral in Hon Sup, Mui Nghe and Mui Gion. In CLC,

427   there was higher coral cover in the south such as in Bai Nan, Bai Huong, Hon Dai and SunGroup
428   than in the north and center of both small and large islands, and Hon Tai in the south.
429
430   Accuracy assessment of the classified images using Maximum Likelihood classifier showed
431   satisfactory performance and a high accuracy in both areas with an overall accuracy of 75% and
432   Kappa coefficients of >0.75. Therefore, the overall approach provides an accessible means for reef
433   scientists and managers to effectively apply remotely sensed data to observe coral ecosystems. The
434   findings of this study can provide a comprehensive understanding of coral pattern and support
435   policymakers/planners to develop appropriate coral reefs conservation policies in coastal regions.
436

437   **Acknowledgements**
438   The authors would like to thank the Planet Education and Research Program for supporting the
439   Planetscope images in this research.
440

441   **References**
442   Ali MZ, Qazi W, Aslam N. 2018. A comparative study of ALOS-2 PALSAR and landsat-8

443   imagery for land cover classification using maximum likelihood classifier. *The Egyptian*

444   *Journal of Remote Sensing and Space Science* 21:S29–S35. DOI:

445   10.1016/j.ejrs.2018.03.003.

446   Anggoro A, Siregar VP, Agus SB. 2016. The effect of sunglint on benthic habitats mapping in Pari

447   Island using worldview-2 imagery. *Procedia Environmental Sciences* 33:487–495. DOI:

448   10.1016/j.proenv.2016.03.101

449   Asner GP, Martin RE, Mascaro J. 2017. Coral reef atoll assessment in the South China Sea using

450   Planet Dove satellites. *Remote Sensing in Ecology and Conservation* 3:57–65. DOI:

451   10.1002/rse2.42

452   Booth DJ, Oldfield RB. 1989. A comparison of classification algorithms in terms of speed and

453   accuracy after the application of a post-classification modal filter. *International Journal of*

454   *Remote Sensing* 10:1271–1276. DOI: 10.1080/01431168908903965

455   Cabral AIR, Silva S, Silva PC, Vanneschi L, Vasconcelos MJ. 2018. Burned area estimations

456   derived from Landsat ETM+ and OLI data: Comparing Genetic Programming with

457   Maximum Likelihood and Classification and Regression Trees. *ISPRS Journal of*

458   *Photogrammetry and Remote Sensing* 142:94–105. DOI: 10.1016/j.isprsjprs.2018.05.007.

459 Capolsini P, Andréfouët S, Rion C, Payri C. 2003. A comparison of Landsat ETM+, SPOT HRV,

460   Ikonos, ASTER, and airborne MASTER data for coral reef habitat mapping in South

461   Pacific islands. *Canadian Journal of Remote Sensing* 29:187–200. DOI: 10.5589/m02-088

462 Carriger JF, Yee SH, Fisher WS. 2021. Assessing coral reef condition indicators for local and

463   global stressors using Bayesian networks. *Integrated Environmental Assessment and*

464   *Management* 17:165–187. DOI: 10.1002/ieam.4368

465 Chou L, Wilkinson CC, Licuanan W, Alino PP, Cheshire AA, Loo M, Tangjaitrong SS, Sudara

466   SS, Ridzwan A, Soekarno SS. 1995. Status of coral reefs in the ASEAN region. In:

467   *Proceedings, Third ASEAN-Australia Symposium on Living Coastal Resources,*

468   *Chulalongkorn University, Bangkok, Thailand, 16-20 May 1994. Volume 1. Status*

469   *Reviews-pages: 1-10.* Australian Institute of Marine Science (AIMS).

470 Gabr B, Ahmed M, Marmoush Y. 2020. PlanetScope and landsat 8 imageries for bathymetry

471   mapping. *Journal of Marine Science and Engineering* 8:143.DOI: 10.3390/jmse8020143

472 Giardino C, Brando VE, Gege P, Pinnel N, Hochberg E, Knaeps E, Reusen I, Doerffer R, Bresciani

473   M, Braga F. 2019. Imaging spectrometry of inland and coastal waters: state of the art,

474   achievements and perspectives. *Surveys in Geophysics* 40:401–429. DOI: 10.1007/s10712-

475   018-9476-0

476 Gonzalez-Rivero M, Beijbom O, Rodriguez-Ramirez A, Bryant DE, Ganase A, Gonzalez-Marrero

477   Y, Herrera-Reveles A, Kennedy EV, Kim CJ, Lopez-Marcano S. 2020. Monitoring of coral

478   reefs using artificial intelligence: A feasible and cost-effective approach. *Remote Sensing*

479   12:489. DOI: 10.3390/rs12030489

480   Goodman J, Purkis S, Phinn S. 2013. *Coral Reef Remote Sensing: A Guide for Mapping,*

481   *Monitoring and Management*. Springer Netherlands. DOI: 10.1007/978-90-481-9292-2.

482   Green E, Mumby P, Edwards A, Clark C. 2000. *Remote sensing: handbook for tropical coastal*

483   *management*. Paris, France: United Nations Educational, Scientific and Cultural

484   Organization (UNESCO).

485   Guan Y, Hohn S, Wild C, Merico A. 2020. Vulnerability of global coral reef habitat suitability to

486   ocean warming, acidification and eutrophication. *Global Change Biology* 26:5646–5660.

487   DOI: 10.1111/gcb.15293

488   Hedberg N, Stenson I, Kautsky N, Hellström M, Tedengren M. 2017. Causes and consequences

489   of spatial links between sea cage aquaculture and coral reefs in Vietnam. *Aquaculture*

490   481:245–254. DOI: 10.1016/j.aquaculture.2017.09.009.

491   Hedley JD, Harborne AR, Mumby PJ. 2005. Simple and robust removal of sun glint for mapping

492   shallow-water benthos. *International Journal of Remote Sensing* 26:2107–2112. DOI:

493   10.1080/01431160500034086

494   Hedley JD, Roelfsema C, Brando V, Giardino C, Kutser T, Phinn S, Mumby PJ, Barrilero O,

495   Laporte J, Koetz B. 2018. Coral reef applications of Sentinel-2: Coverage, characteristics,

496   bathymetry and benthic mapping with comparison to Landsat 8. *Remote sensing of*

497   *environment* 216:598–614. DOI: 10.1016/j.rse.2018.07.014

498   Hedley JD, Roelfsema CM, Chollett I, Harborne AR, Heron SF, Weeks S, Skirving WJ, Strong

499   AE, Eakin CM, Christensen TR. 2016. Remote sensing of coral reefs for monitoring and

500   management: a review. *Remote Sensing* 8:118. DOI: 10.3390/rs8020118

501   Hill J, Wilkinson C. 2004. *Methods for ecological monitoring of coral reefs*. Australian Institute

502   of Marine Science, Townsville 117.

503 Hoang MD, Tran VB, Le D, To VQ, Hoang QH. 2019. Distribution of terrestrial fauna on Son Tra
504   Peninsula, Da Nang City. *The University of Danang, Journal of Science and Technology*
505   17:34–39. DOI: 10.31130/jst-ud2019-116e.

506 Hochberg EJ, Andréfouët S, Tyler MR. 2003. Sea surface correction of high spatial resolution
507   Ikonos images to improve bottom mapping in near-shore environments. *IEEE transactions*
508   *on geoscience and remote sensing* 41:1724–1729. DOI: 10.1109/TGRS.2003.815408

509 Hoegh-Guldberg O, Pendleton L, Kaup A. 2019. People and the changing nature of coral reefs.
510   *Regional Studies in Marine Science* 30:100699. DOI: 10.1016/j.rsma.2019.100699

511 Hua TT, Vo ST, Phan KH, Huynh ND. 2015. Survival and growth rate of hard corals rehabilitated
512   in Cu Lao Cham marine protected area, Quang Nam province. *Collection of Marine*
513   *Research Works* 21:94–102.

514 Kay S, Hedley JD, Lavender S. 2009. Sun Glint Correction of High and Low Spatial Resolution
515   Images of Aquatic Scenes: a Review of Methods for Visible and Near-Infrared
516   Wavelengths. *Remote Sensing* 1:697–730. DOI: 10.3390/rs1040697.

517 Kimura T, Tun K, Chou L. 2014. *Status of Coral Reefs in East Asian Seas Region: 2014*. Tokyo,
518   Japan: Ministry of the Environment of Japan and Japan Wildlife Research Center.

519 Kimura T, Tun K, Chou L. 2018. *Status of Coral Reefs in East Asian Seas Region: 2018*. Tokyo,
520   Japan: Ministry of the Environment of Japan and Japan Wildlife Research Center.

521 Kohler KE, Gill SM. 2006. Coral Point Count with Excel extensions (CPCe): A Visual Basic
522   program for the determination of coral and substrate coverage using random point count
523   methodology. *Computers & geosciences* 32:1259–1269.
524   DOI:10.1016/j.cageo.2005.11.009

525 Latypov YuYa, Selin NI. 2008. Coral communities of barrier reefs of Vietnam. *Russian Journal*

526   *of Marine Biology* 34:143–150. DOI: 10.1134/S1063074008030012.

527 Lazuardi W, Wicaksono P, Marfai MA. 2021. Remote sensing for coral reef and seagrass cover

528   mapping to support coastal management of small islands. In: *IOP Conference Series: Earth*

529   *and Environmental Science*. IOP Publishing, 012031. DOI: 10.1088/1755-

530   1315/686/1/012031

531 Le DD. 2020. The status of coral reefs in central Vietnam's coastal water under climate change.

532   *Aquatic Ecosystem Health & Management* 23:323–331. DOI:

533   10.1080/14634988.2020.1819715

534 Leiper IA, Phinn SR, Roelfsema CM, Joyce KE, Dekker AG. 2014. Mapping coral reef benthos,

535   substrates, and bathymetry, using compact airborne spectrographic imager (CASI) data.

536   *Remote Sensing* 6:6423–6445. DOI: 10.3390/rs6076423

537 Lemajic S, Vajsová B, Aastrand P. 2018. *New Sensors Benchmark Report on PlanetScope:*

538   *Geometric Benchmarking Test for Common Agricultural Policy (CAP) Purposes*.

539   European Commission: Brussels, Belgium. DOI: 10.2760/178918

540 Levy J, Hunter C, Lukacazyk T, Franklin EC. 2018. Assessing the spatial distribution of coral

541   bleaching using small unmanned aerial systems. *Coral Reefs* 37:373–387. DOI:

542   10.1007/s00338-018-1662-5

543 Li J, Schill SR, Knapp DE, Asner GP. 2019. Object-based mapping of coral reef habitats using

544   planet dove satellites. *Remote Sensing* 11:1445. DOI: 10.3390/rs11121445

545 Lillesand T, Kiefer RW, Chipman J. 2015. *Remote sensing and image interpretation*. John Wiley

546   & Sons, Hoboken, NJ 07030-5774.

547   Lyzenga DR. 1978. Passive remote sensing techniques for mapping water depth and bottom

548   features. *Applied optics* 17:379–383.DOI: 10.1364/AO.17.000379

549   Lyzenga DR. 1981. Remote sensing of bottom reflectance and water attenuation parameters in

550   shallow water using aircraft and Landsat data. *International journal of remote sensing*

551   2:71–82. DOI: 10.1080/01431168108948342

552   Mansaray AS, Dzialowski AR, Martin ME, Wagner KL, Gholizadeh H, Stoodley SH. 2021.

553   Comparing PlanetScope to Landsat-8 and Sentinel-2 for Sensing Water Quality in

554   Reservoirs in Agricultural Watersheds. *Remote Sensing* 13:1847. DOI:

555   10.3390/rs13091847

556   McCarthy MJ, Colna KE, El-Mezayen MM, Laureano-Rosario AE, Méndez-Lázaro P, Otis DB,

557   Toro-Farmer G, Vega-Rodriguez M, Muller-Karger FE. 2017. Satellite remote sensing for

558   coastal management: A review of successful applications. *Environmental management*

559   60:323–339. DOI: 10.1007/s00267-017-0880-x

560   McHugh ML. 2012. Interrater reliability: the kappa statistic. *Biochemia Medica* 22:276–282.

561   Mumby PJ, Edwards AJ. 2002. Mapping marine environments with IKONOS imagery: enhanced

562   spatial resolution can deliver greater thematic accuracy. *Remote sensing of environment*

563   82:248–257. DOI: 10.1016/S0034-4257(02)00041-X

564   Mumby PJ, Skirving W, Strong AE, Hardy JT, LeDrew EF, Hochberg EJ, Stumpf RP, David LT.

565   2004. Remote sensing of coral reefs and their physical environment. *Marine pollution*

566   *bulletin* 48:219–228. DOI: 10.1016/j.marpolbul.2003.10.031

567   Nguyen VL. 2009. Coral reef fishes in the coastal waters of south-central Vietnam. *Vietnam*

568   *Journal of Marine Science and Technology* 9. DOI: 10.15625/1859-3097/9/3/6273

569   Nguyen XT, Bui TBA, Nguyen TN. 2019. Research on marine environment and coral distribution

570   on Nam Yet island using VNRedsat-1 and QuickBird images. *Vietnam Journal of Marine*

571   *Science and Technology* 19:189–202. DOI: 10.15625/1859-3097/19/3B/14525

572   Nguyen XT, Dang TBA, Nguyen TN, Pham DH. 2019a. Study on spatial distribution of coral reefs

573   in Nam Yet island by using GIS and remote sensing techniques. *Vietnam Journal of Marine*

574   *Science and Technology* 19:177–187. DOI: 10.15625/1859-3097/19/3B/14524

575   Nguyen T, Huynh T, Zhang H. 2015. Cu Lao Cham biosphere reserve sustainability project In

576   Vietnam: corporate framework for sustainable development management. *Sustainable*

577   *Development (2 Volume Set)* 168:115. DOI: 10.2495/SD150021

578   Nguyen HQ, Luong VT, Ho DD. 2015. Study on spatial distribution of coral reefs in Ly Son Island

579   using GIS and remote sensing technique. *Vietnam Journal of Marine Science and*

580   *Technology* 15:264–272. DOI: 10.15625/1859-3097/15/3/7222

581   Nguyen QC, Nguyen VC. 2014. Integrated coastal management in Vietnam: current situation and

582   orientation. *Vietnam Journal of Marine Science and Technology* 14:89–96.

583   DOI:10.15625/1859-3097/14/1/4034

584   Nguyen TTH, Nguyen TH, Nguyen VT, Nguyen NL. 2019a. Spatial distribution of submerged

585   aquatic vegetation in An Chan coastal waters, Phu Yen province using the PlanetScope

586   satellite image. *Vietnam Journal of Earth Sciences* 41:358–373. DOI: 10.15625/0866-

587   7187/41/4/14237

588   Nguyen TTH, Nguyen TH, Tong PHS, Nguyen NL. 2019b. Vegetation Biomass of Sargassum

589   Meadows in An Chan Coastal Waters, Phu Yen Province, Vietnam Derived from

590   PlanetScope Image. *Journal of Environmental Science and Engineering* 8:81–92. DOI:

591   :10.17265/2162-5263/2019.03.001

592   Nguyen VL, Phan HK. 2008. Distribution and factors influencing on structure of reef fish

593   communities in Nha Trang Bay Marine Protected Area, South-Central Vietnam.

594   *Environmental biology of fishes* 82:309–324. DOI: 10.1007/s10641-007-9293-7

595   Nguyen VL, Vo ST. 2013. Degradation trend of coral reefs in the coastal waters of Vietnam.

596   *Galaxea, Journal of Coral Reef Studies* 15:79–83. DOI: 10.3755/galaxea.15.79.

597   Obura DO, Aeby G, Amornthammarong N, Appeltans W, Bax N, Bishop J, Brainard RE, Chan S,

598   Fletcher P, Gordon TA. 2019. Coral reef monitoring, reef assessment technologies, and

599   ecosystem-based management. *Frontiers in Marine Science* 6:580. DOI:

600   10.3389/fmars.2019.00580

601   Pahlevan N, Valadanzouj MJ, Alimohamadi A. 2006. A quantitative comparison to water column

602   correction techniques for benthic mapping using high spatial resolution data. In:

603   *Proceedings of the ISPRS Commission VII Mid-term Symposium―Remote Sensing, from*

604   *Pixels to Processes‖, Enschede, The Netherlands*. Citeseer, 8–11.

605   Pawlik JR, McMurray SE. 2020. The emerging ecological and biogeochemical importance of

606   sponges on coral reefs. *Annual review of marine science* 12:315–337. DOI:

607   10.1146/annurev-marine-010419-010807

608   Phinn SR, Roelfsema CM, Mumby PJ. 2012. Multi-scale, object-based image analysis for mapping

609   geomorphic and ecological zones on coral reefs. *International Journal of Remote Sensing*

610   33:3768–3797. DOI: 10.1080/01431161.2011.633122

611   Pu R, Bell S, Meyer C, Baggett L, Zhao Y. 2012. Mapping and assessing seagrass along the

612   western coast of Florida using Landsat TM and EO-1 ALI/Hyperion imagery. *Estuarine,*

613   *Coastal and Shelf Science* 115:234–245. DOI: 10.1016/j.ecss.2012.09.006

614 Quach TKN. 2018. Impacts on the ecosystem and human well-being of the marine protected area

615   in Cu Lao Cham, Vietnam. *Marine Policy* 90:174–183. DOI:

616   10.1016/j.marpol.2017.12.015.

617 Richards JA. 1999. *Remote sensing digital image analysis*. Berlin, Germany: Springer.

618 Roelfsema CM, Phinn SR, Joyce KE. 2006. Evaluating benthic survey techniques for validating

619   maps of coral reefs derived from remotely sensed images. In: *Proc 10th Int Coral Reef*

620   *Symp*. Citeseer, 1771–1780.

621 Tobler, W.R. (1988) Resolution, resampling and all that. In Mounsey, H. and Tomlinson, R.,

622   Editors, Building Databases for Global Science. London: Taylor and Francis, p.129-137.

623 Tran VD, Phinn S, Roelfsema C. 2012. Coral Reef Mapping in Vietnam's Coastal Waters from

624   High-spatial Resolution Satellite and Field Survey Data. *Asian Journal of Geoinformatics*

625   12.

626 Tun K, Chou LM, Yeemin T, Phongsuwan N, Amri AY, Ho N, Sour K, Long N, Nanola C, Lane

627   D. 2008. Status of coral reefs in Southeast Asia. In: *Status of coral reefs of the world*.

628   Townsville: Australian Institute of Marine Science, 131–144.

629 Wang M, Bailey SW. 2001. Correction of sun glint contamination on the SeaWiFS ocean and

630   atmosphere products. *Applied Optics* 40:4790–4798. DOI: 10.1364/AO.40.004790

631 Wicaksono P, Lazuardi W. 2018. Assessment of PlanetScope images for benthic habitat and

632   seagrass species mapping in a complex optically shallow water environment. *International*

633   *journal of remote sensing* 39:5739–5765. DOI: 10.1080/01431161.2018.1506951

634 Wulandari SA, Wicaksono P. 2021. Bathymetry mapping using PlanetScope imagery on Kemujan

635   Island, Karimunjawa, Indonesia. In: *IOP Conference Series: Earth and Environmental*

636   *Science*. IOP Publishing, 012032.

637   Yamano H, Tamura M. 2004. Detection limits of coral reef bleaching by satellite remote sensing:

638   simulation and data analysis. *Remote sensing of environment* 90:86–103. DOI:

639   10.1016/j.rse.2003.12.005

640   Zhou Z, Ma L, Fu T, Zhang G, Yao M, Li M. 2018. Change Detection in Coral Reef Environment

641   Using High-Resolution Images: Comparison of Object-Based and Pixel-Based Paradigms.

642   *ISPRS International Journal of Geo-Information* 7:441. DOI: 10.3390/ijgi7110441.

643   Zoffoli ML, Frouin R, Kampel M. 2014. Water Column Correction for Coral Reef Studies by

644   Remote Sensing. *Sensors* 14:16881–16931. DOI: 10.3390/s140916881.

645

646

Figure 1

Location of study area (a) Son Tra Peninsula (ST) and (b) Cu Lao Cham Island (CLC).
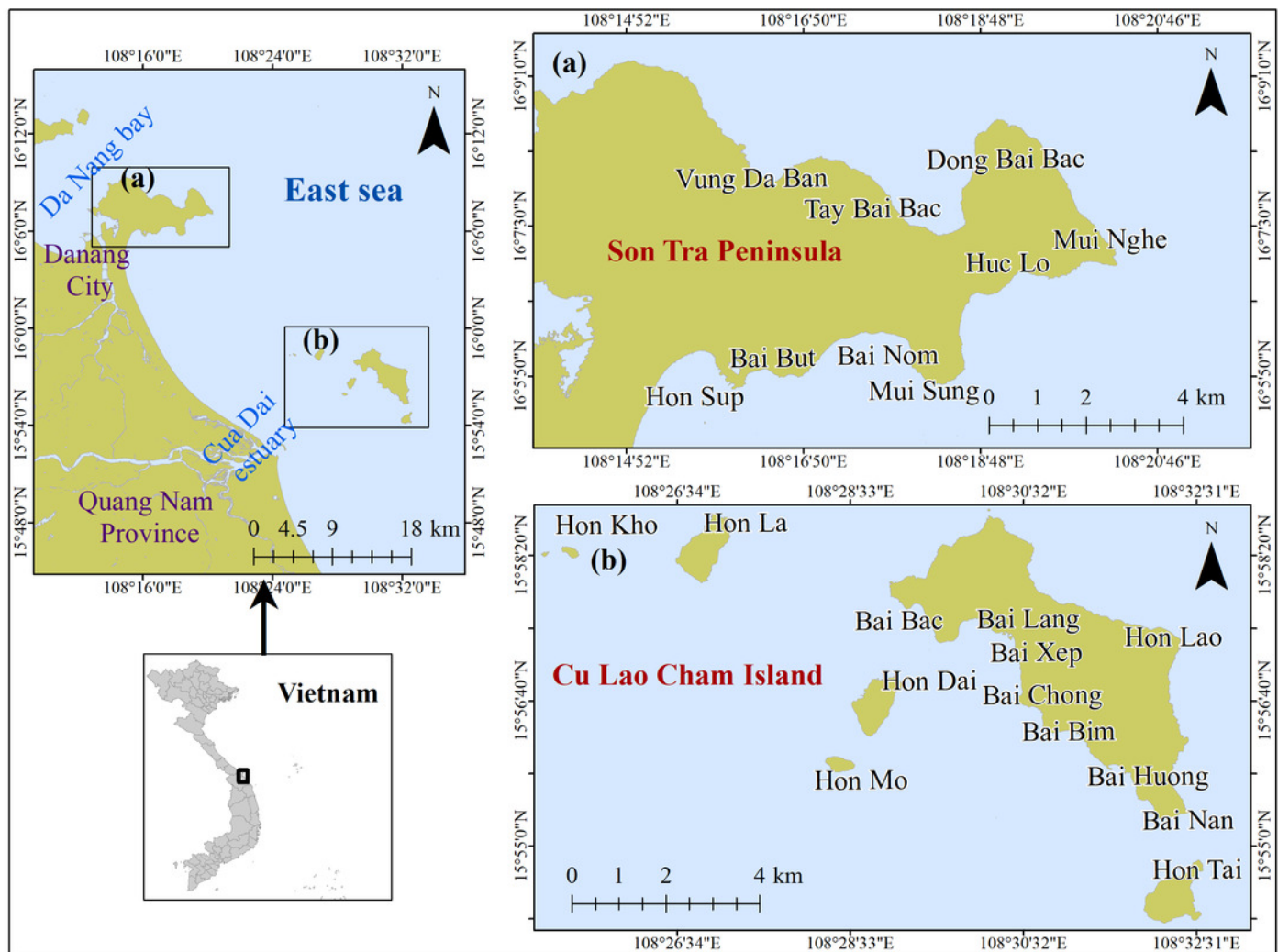
Figure 2

Flowchart of coral distribution mapping in the study area.
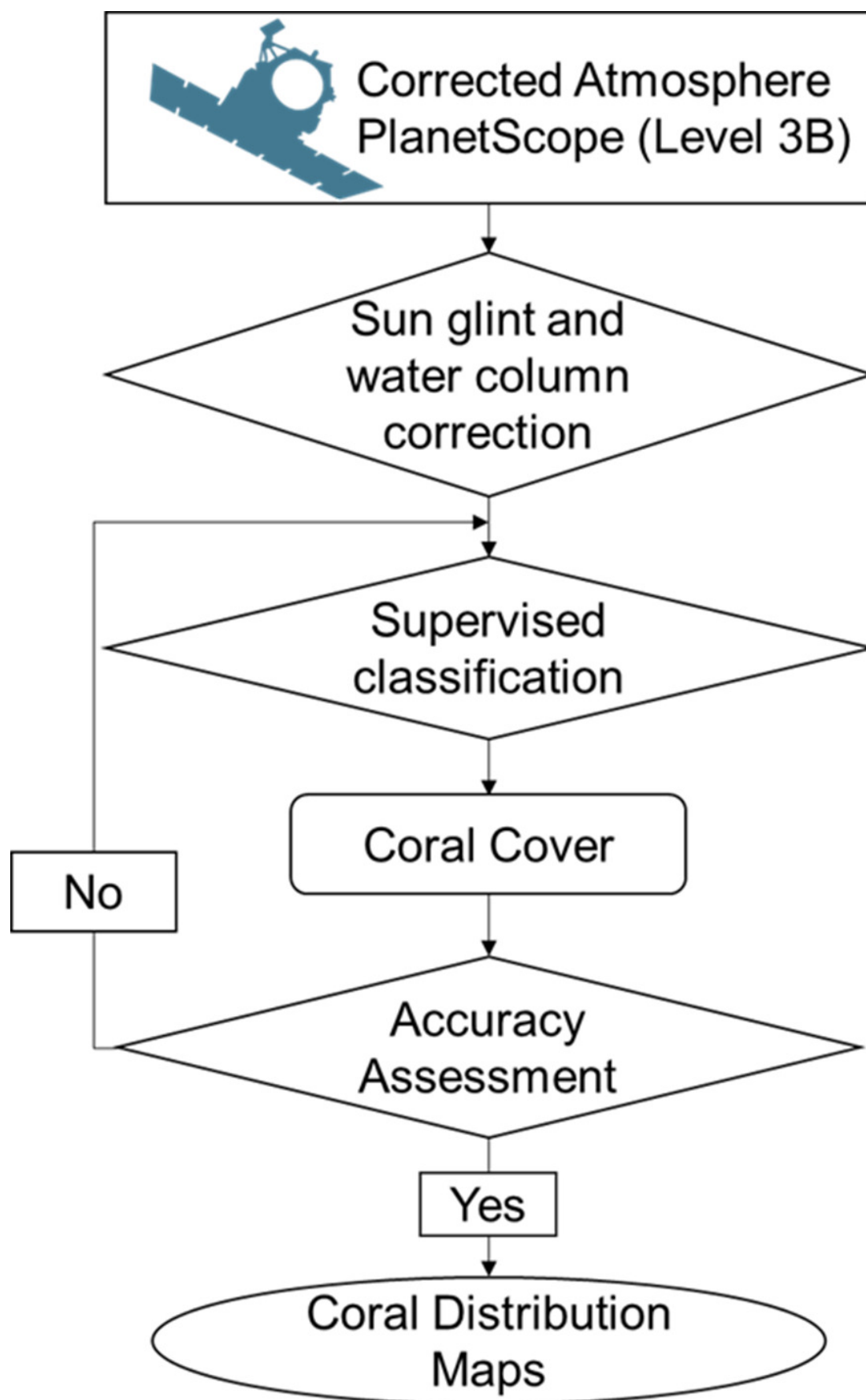
Figure 3

Transformed band ratios of Planetscope bands in ST [(a) bands 1 and 2, (b) bands 2 and 3, and (c) bands 1 and 3] and in CLC [(d) bands 1 and 2 (e) bands 2 and 3, and (f) bands 1 and 3].
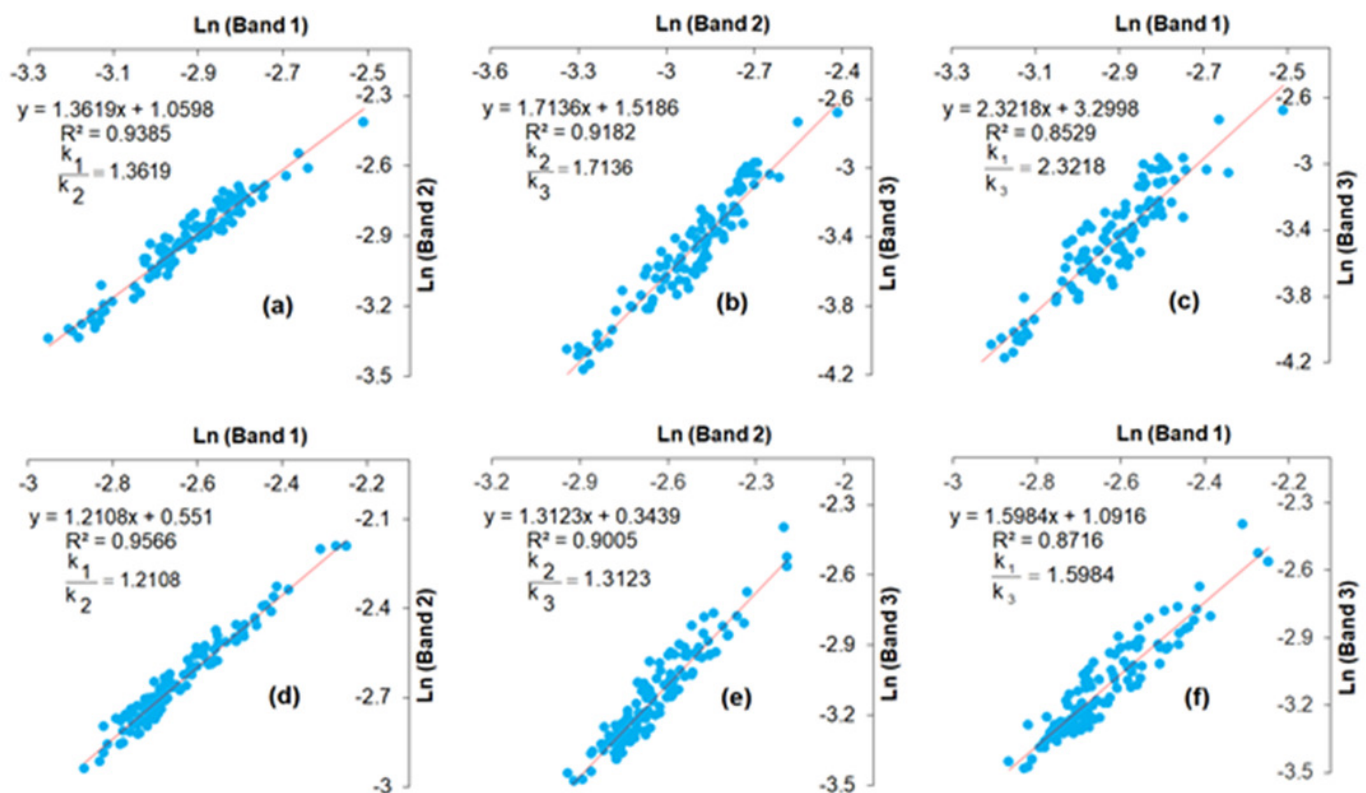
Figure 4

Spectral signatures of (a) six classes at ST and (b) seven classes at CLC.
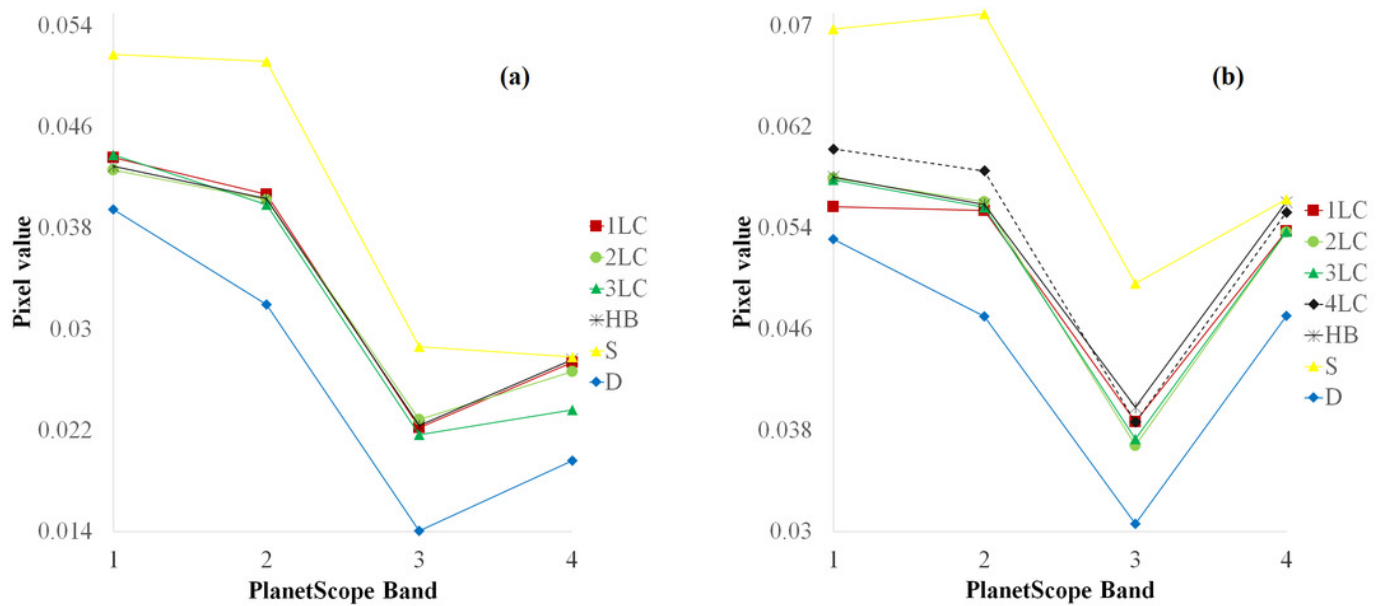
Figure 5

Depth histogram of coral distribution in (a) Son Tra Peninsula and (b) Cu Lao Cham Island.
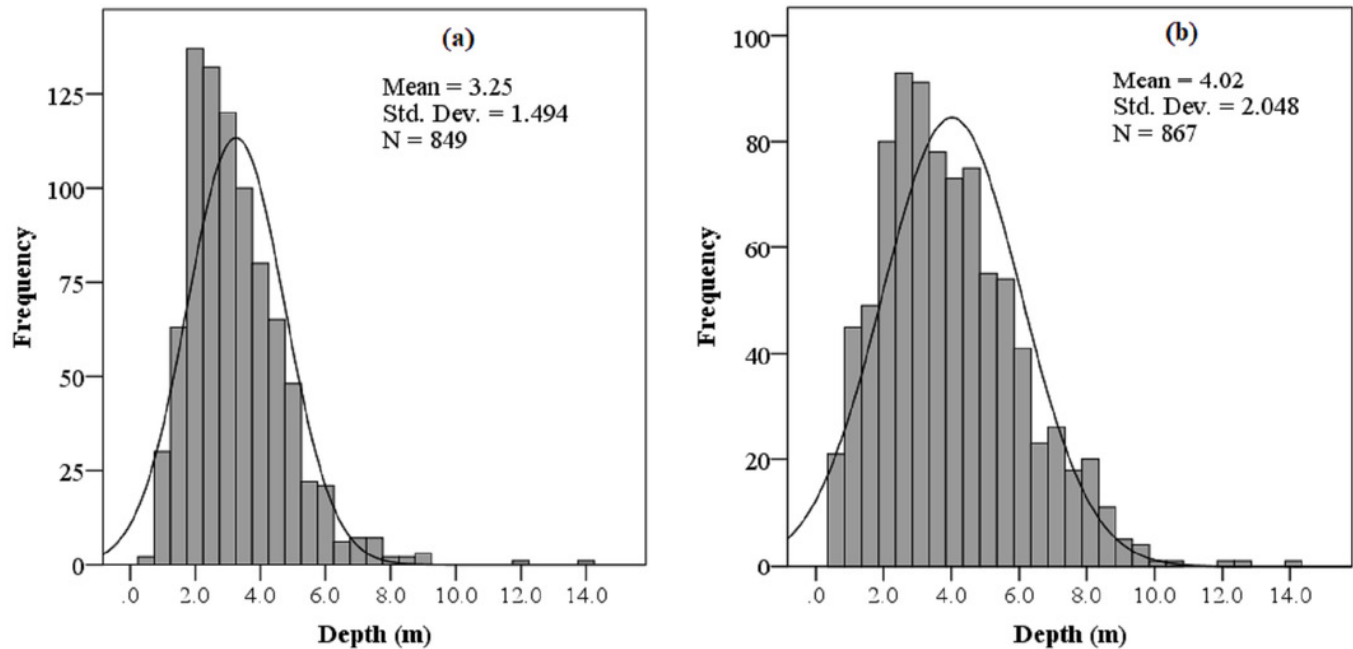
Figure 6

Coral cover in Son Tra Peninsula.

1LC: Poor; 2LC: Fair; 3LC: Good; S: Sand; and HB: Hard bottom
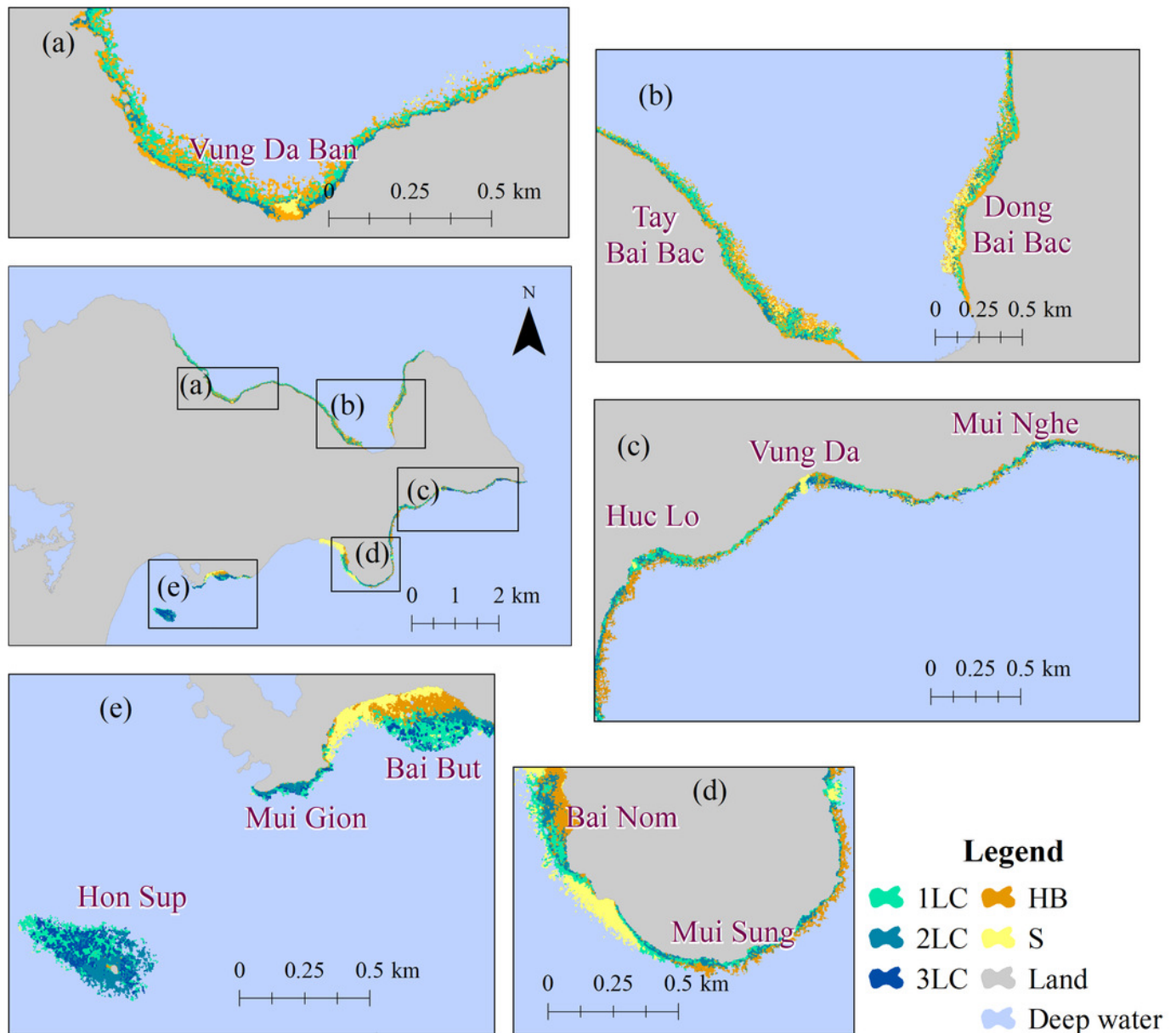
Figure 7

Coral cover in Cu Lao Cham Island.

1LC: Poor; 2LC: Fair; 3LC: Good; 4LC: Excellent; S: Sand; and HB: Hard bottom
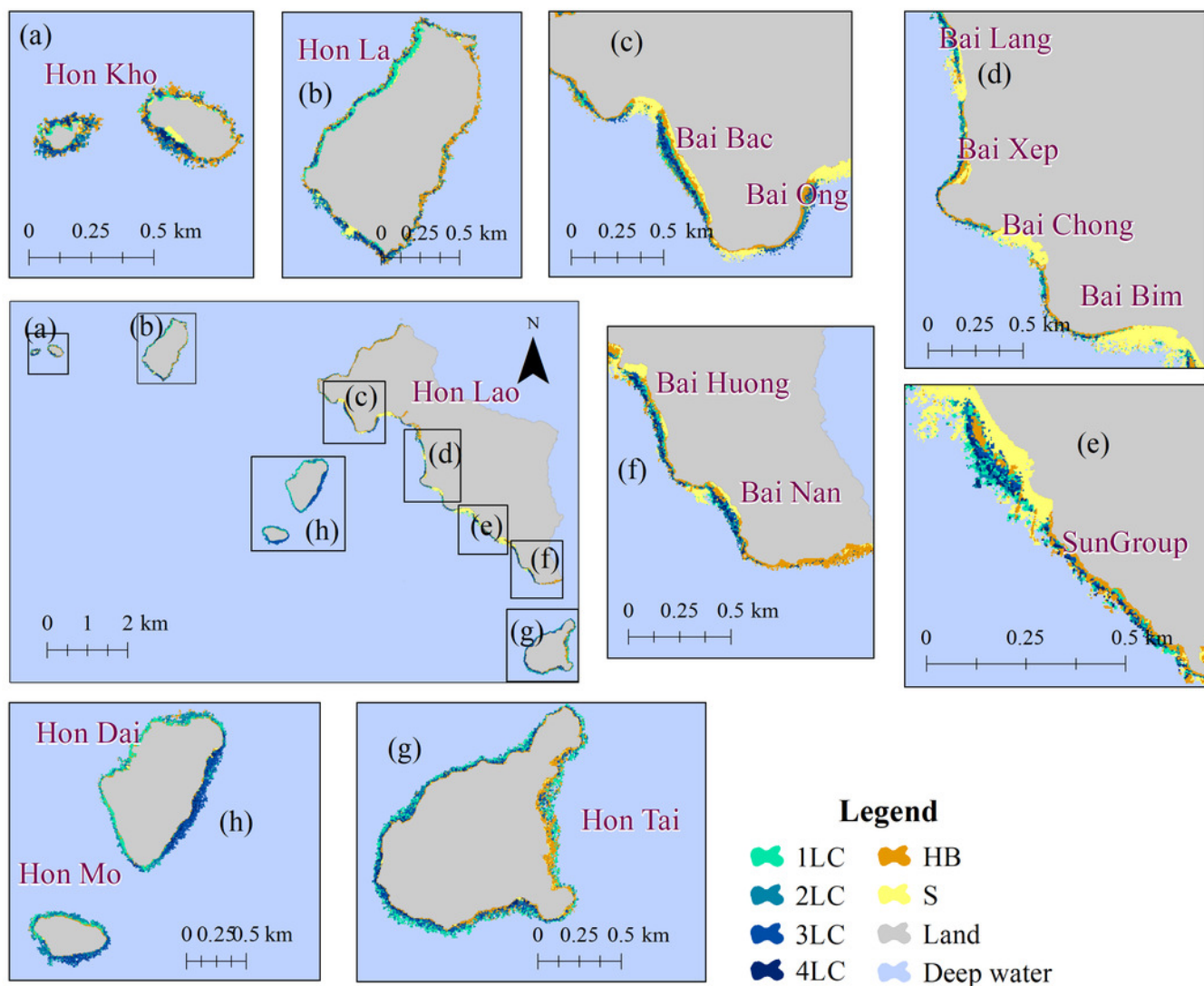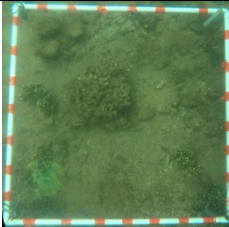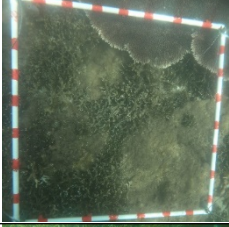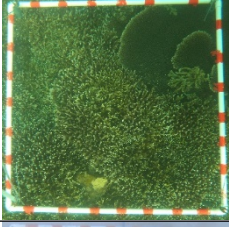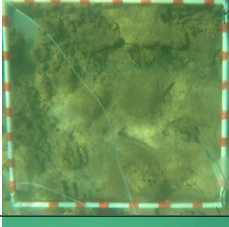
Details of the acquired Planetscope imagery.

Location	Row	Path	Data of Acquisition	Spatial resolution
Son Tra	021	858	28 June 2019	
		859		3 m
Cu Lao Cham	025	351	08 August 2019	
		352		

Identification scheme of bottom types and coral reef health.

Class	Detail	Class description	Coral reef health criteria	Label	Depth range (m)	Sample image
Live coral (LC)	hard and soft coral	$0 < LC \leq 25\%$	Poor	1LC	ST: 0.8 – 8.5 CLC: 0.6 – 11.5	
		$25 < LC \leq 50\%$	Fair	2LC	ST: 0.5-8.2 CLC: 0.9 – 9.9	
		$50 < LC \leq 75\%$	Good	3LC	ST: 1.3 – 7 CLC: 0.8 – 10.2	
		$LC > 75\%$	Excellent	4LC	CLC: 0.9 – 10.5	
Sand (S)	Sand dominated	$LC = 0\%$ and $S \geq 50\%$ S		S	ST: 0.5 – 13.1 CLC: 0.4 – 12.5	
Hard bottom	Rock, rubble, dead structure	$LC = 0\%$ LC and $HB > 50\%$		HB	ST: 1 – 8.2 CLC: 0.7 – 10.5	
Deep zone		Depth > 14 m		D	ST: 14 – 24 CLC: 14 – 29.5	

Interpretation of Kappa values.

Value	Description
Less than 0	Less than chance agreement
0.01-0.2	Sigh agreement
0.21-0.40	Fair agreement
0.41-0.60	Moderate agreement
0.61-0.80	Substantial agreement
0.81-1.00	Almost perfect agreement

Percentage of coral cover classes in the coral reefs of Son Tra Peninsula and Cu Lao Cham Island.

Location	Level (%)	1LC	2LC	3LC	4LC
Son Tra	Vung Da Ban	75.19	24.81	-	-
	Tay Bai Bac - Dong Bai Bac	71.05	28.95	-	-
	Mui Nghe – Huc Lo	48.68	38.06	13.26	-
	Mui Sung – Bai Nom	59.48	40.52	-	-
	Bai But – Hon Sup	46.51	33.76	19.73	-
	Total	**60.25**	**31.88**	**7.87**	**-**
Cu Lao Cham	Hon Kho	20.15	36.26	30.42	13.17
	Hon La	42.08	28.21	22.67	7.04
	North of main island (NI) to Bai Ong	15.54	54.31	25.76	4.39
	Harbour – Bai Bim	32.87	38.29	21.46	7.38
	SunGroup	45.1	13.49	25.26	16.15
	Bai Huong – Bai Nan	33.54	19.15	25.98	21.33
	Hon Tai	46.26	19.7	26.81	7.23
	Hon Mo – Hon Dai	31.59	23.78	27.07	17.56
	Total	**34.28**	**28.51**	**25.75**	**11.46**

Confusion matrix of bottom types in Son Tra Peninsula.

Class	1LC	2LC	3LC	HB	S	D	Total	UA
1LC	**49**	5	3	7	3	2	69	**71.01**
2LC	5	**44**	10	3	1	1	64	**68.75**
3LC	1	7	**38**	1	0	0	47	**80.85**
HB	6	0	0	**32**	3	2	43	**74.42**
S	1	0	0	3	**41**	6	51	**80.39**
D	2	0	1	1	1	**44**	49	**89.8**
Total	64	56	52	47	49	55	**OV**	76.78
PA	**76.56**	**78.57**	**73.08**	**68.09**	**83.67**	**80**	**KC**	**0.76**

Confusion matrix of bottom types in Cu Lao Cham Island.

Class	1LC	2LC	3LC	4LC	HB	S	D	Total	UA
1LC	**47**	7	1	3	2	1	1	62	**75.81**
2LC	3	**46**	5	2	0	0	0	56	**82.14**
3LC	0	7	**43**	3	1	0	0	54	**79.63**
4LC	0	4	5	**40**	6	0	0	55	**72.73**
HB	5	4	2	0	**30**	1	1	43	**69.77**
S	0	2	0	0	6	**43**	4	55	**78.18**
D	1	2	0	0	2	0	**39**	44	**88.64**
Total	56	72	56	48	47	45	45	**OV**	78.05
PA	**84**	**63.89**	**76.79**	**83.33**	**63.83**	**95.56**	**86.67**	**KC**	**0.78**